

## Notes &amp; Tips

## Method for estimating the single molecular affinity

Richard B.M. Schasfoort<sup>a,b,\*</sup>, Wim de Lau<sup>c</sup>, Alex van der Kooi<sup>b</sup>, Hans Clevers<sup>c</sup>, Gerard H.M. Engbers<sup>b</sup><sup>a</sup> Medical Cell Biophysics Group, MIRA Institute, University of Twente, 7500 AE Enschede, The Netherlands<sup>b</sup> IBIS Technologies, 7521 PR Enschede, The Netherlands<sup>c</sup> Hubrecht Institute and University Medical Center Utrecht, 3584 CX Utrecht, The Netherlands

## ARTICLE INFO

## Article history:

Received 30 September 2011

Received in revised form 1 December 2011

Accepted 5 December 2011

Available online 13 December 2011

## Keywords:

Label free

Protein interaction analysis

Kinetics

Rate and dissociation equilibrium constants

SPR imaging

## ABSTRACT

Affinity constants ( $k_d$ ,  $k_a$ , and  $K_D$ ) can be determined by methods that apply immobilized ligands such as immunoassays and label-free biosensor technologies. This article outlines a new surface plasmon resonance (SPR) array imaging method that yields affinity constants that can be considered as the best estimate of the affinity constant for single biomolecular interactions. Calculated rate ( $k_d$  and  $k_a$ ) and dissociation equilibrium ( $K_D$ ) constants for various ligand densities and analyte concentrations are extrapolated to the  $K_D$  at the zero response level ( $K_D^{RO}$ ). By applying this method to an LGR5-exo-Fc-RSPO1-FH interaction couple, the  $K_D^{RO}$  was determined as 3.1 nM.

© 2011 Elsevier Inc. All rights reserved.

For multiple applications, the quality of binding, expressed as the dissociation equilibrium constant ( $K_D$ ), is of great importance because it determines, for instance, the relevant concentration range of therapeutics in immune therapy. The  $K_D$  value (M, mol/L) is the analyte concentration at which in equilibrium 50% of the ligand molecules are bound. The majority of methods for the determination of affinity constants are based on assays in which the interaction occurs at surfaces such as surface plasmon resonance (SPR),<sup>1</sup> bilayer interferometry, and quartz crystal microbalance. Because the  $K_D$  is used for the determination of the effective dosage levels of biomolecules that are applied as drugs, the determined  $K_D$  should reflect the  $K_D$  in solution. However, the constants that are derived from current immobilized ligand-based assays are affected by the immobilized state of the ligand [1]. This causes the determined apparent constants to deviate from the true “solution” constants due to interfering effects that result from the immobilized status of the ligand. Some of these interfering effects include rebinding effects, mass transport limitation, nonspecific binding, and deviation from 1:1 model binding [2,3]. The higher the ligand density, the more pronounced these interfering effects become, and it is generally accepted that the ligand density should be applied just above the limit of detection of the biosensor instrument. However, even at

low responses, the interfering effects may occur substantially. The same holds for the analyte concentration; interfering effects will occur when multiple analyte molecules compete for interaction with a single immobilized ligand molecule.

This article introduces a new method for the determination of affinity constants in which the contribution of interfering effects is minimized or theoretically zeroed, so that the constants are a better estimate of the true constants of biomolecular interactions in solution. The method is based on the extrapolation of the number of immobilized ligand and analyte molecules to zero, thereby mimicking the interaction in which only one ligand and one analyte molecule are involved, enabling a true 1:1 binding model without or with minimal interfering effects. The method is presented by determination of the affinity constant for the LGR5-exo-Fc-RSPO1-FH interaction using array imaging SPR as the detection technique [4].

Although this extrapolation method was recently applied for the first time in a study by de Lau and coworkers [4], it was not explained in that article why the method is the strategy of choice for determining the affinity constants as a quality parameter of interacting molecules. That is the aim of the current article. Generally when multiple immobilized ligand molecules are present in a certain density and analyte molecules are present in a certain concentration, always this will result in more or less interfering effects. These interfering effects can be grouped as follows:

- (1) Parallel binding processes, including nonspecific binding and/or cross-reactivity, dimerization, and formation of multi-assembly complexes.

\* Corresponding author at: Medical Cell Biophysics Group, MIRA Institute, University of Twente, 7500 AE Enschede, The Netherlands. Fax: +31 53 475 1856.

E-mail address: [r.b.m.schasfoort@utwente.nl](mailto:r.b.m.schasfoort@utwente.nl) (R.B.M. Schasfoort).

<sup>1</sup> Abbreviations used: SPR, surface plasmon resonance; FH, Flag-HA; HSA, human serum albumin.

- (2) Rebinding of dissociating analyte molecules.
- (3) Steric hindrance and/or “avidity” effects.
- (4) Non-1:1-binding model interactions, including biphasic behavior and bridging by molecules having more than one paratope.
- (5) Ligand immobilization artifacts and heterogeneity of surface binding sites [3].
- (6) Mass transport limitation effects (e.g., analyte depletion of the layer close to the immobilized ligand surface).
- (7) Additional interfering effects that do not fit into one of these groups such as complex reactions (e.g., induced fit, allosteric conformational change).

As already indicated, the calculation of the “real” dissociation equilibrium constant  $K_D$  will become more reliable at lower ligand densities, preferably at a density of only a single immobilized ligand molecule acting as a free ligand. Then the contribution of the interfering effects will be zero and will not influence the rate and dissociation equilibrium constants anymore. This situation can be simulated by exposing spots with different ligand concentrations to solutions with different analyte concentrations and then extrapolating the responses to a ligand density and analyte concentration of zero. It should be noted that immobilization artifacts and heterogeneity of surface binding sites can be prevented, for instance, by oriented capturing of the ligands by applying high-affinity anti-ligand antibodies or using tag–anti-tag interactions as shown in this article.

In a favorable experimental design, an array of spots with various anti-ligand densities is first brought into contact with the high-affinity ligand and subsequently with serially diluted analyte solutions automatically. The ligand–analyte interaction is determined to be label free, for instance, by imaging SPR. The flow rates should be sufficiently high to prevent mass transport from becoming a limiting factor. Then the rate and dissociation equilibrium constants can be calculated from a limited number of experiments. This experimental design was applied for the determination of the rate and dissociation equilibrium constants for the LGR5-exo-Fc–RSPO1-FH interaction using array imaging SPR as the detection technique.

Recently, it was shown that soluble RSPO1 binds specifically to LGR4/5/6 family members, which are facultative Wnt receptor components that mediate RSPO1 signaling [4]. Although RSPO1 has been reported to be a high-affinity ligand of the Wnt coreceptor Lrp6 [5], the effective concentration was determined experimentally. A double (Flag–HA)-tagged version of human RSPO1 (RSPO1-FH) produced the optimal effective concentration of approximately 1  $\mu\text{g}/\text{ml}$  in HEK293T cells. Soluble RSPO1-FH interacted with the leucine-rich repeat exodomain of LGR5 [4], expressed as an IgG-Fc fusion protein (LGR5-exo-Fc), and the specific detection was revealed in a binding experiment using SPR array imaging [4,6].

For the SPR imaging experiment, an Easy2Spot sensor chip (IBIS Technologies, Enschede, The Netherlands) was spotted using a Continuous Flow Microspotter (Wasatch Microfluidics, Salt Lake City, UT, USA). In total, 36 spots were created with mouse anti-Flag, goat anti-human IgG-Fc, and mouse anti-HA tag in an  $8 \times$  serial dilution (start concentrations were 500 and 100  $\mu\text{g}/\text{ml}$ ) in 10 mM Mes buffer (pH 5.5). (See the inset of Fig. 1 for an SPR image of a typical 48-plex sensor chip.) Control (reference) spots contained human serum albumin (HSA) or anti-HSA or were “empty.” These reference spots were also used to compensate for bulk refractive index steps. Samples were exposed to all of these spots at the same time, so that interactions were followed in a 36-plex format. After spotting, the sensor chip was positioned in an IBIS MX96 instrument (IBIS Technologies) for label-free SPR array analysis. Detailed operation of the predecessor of the IBIS MX96 instrument and the Continuous Flow Microspotter have been described elsewhere [7,8].

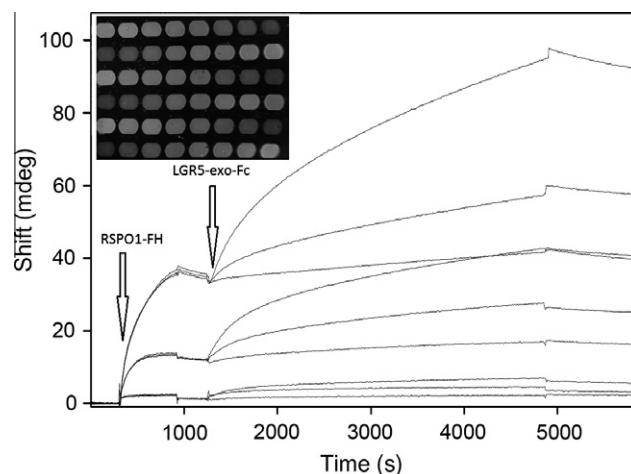


**Fig. 1.** A typical SPR overlay plot showing the loading of RSPO1-FH (300–900 s) on three spots with decreasing anti-Flag antibody densities ( $R_{\text{RSPO1}}$  values of  $\sim 35$ , 12, and 2 mdeg) followed by three injections of LGR5-exo-Fc in serial dilution starting at 45 nM. The results of only three spots are shown for clear presentation, but the results of all eight spots were used to calculate the  $k_d^{\text{RO}}$  and  $K_D^{\text{RO}}$  values. Inset: Typical SPR image of 48 spots in a  $6 \times 8$  ligand density array printed by a Continuous Flow Microspotter.

The anti-Flag and anti-HA spots readily captured RSPO1-FH proportional to the anti-Flag/anti-HA density. Analogously anti-Fc spots captured the Fc tag of LGR5-exo-Fc, and the binding process could be followed in real time. The response  $R_{\text{RSPO1}}$  (or  $R_L$ ) was measured on the various anti-Flag spots with decreased density of anti-Flag antibodies followed by dissociation and injection of the analyte LGR5-Fc or Noggin-Fc into culture supernatants. After a wash, LGR5-exo-Fc bound to the captured RSPO1-FH specifically. At the same time, the LGR5-exo-Fc was binding to an anti-Fc spot. After ligand capturing and serial interactions, the sensor chip was cleaned with regeneration buffer (Gly–HCl, 10 mM, pH 2.0), ending the first step of the analysis cycle. The next step of the analysis cycle was loading the sensor chip with undiluted RSPO1 followed by injecting a  $2 \times$  diluted LGR5-exo-Fc analyte solution, regeneration, and so forth. At least 25 analysis cycles, including controls, were performed automatically. In this way, sensorgrams for interactions of high to low RSPO1 ligand density and high to low LGR5-exo-Fc analyte concentrations are obtained. In Fig. 1, the interactions for three representative spots with different ligand densities and three analyte concentrations are shown.

Fig. 2A and B show the respective graphs of  $k_d$  and  $K_D$  versus  $R_L$ .  $R_L$  is the response of ligand capturing and corresponds to the number of analyte binding sites per spot. The data points are fitted with the exponential equation  $y = a^x e^{bx}$ . By extrapolation of  $R_L = x$  to 0, rate constants  $k_d^{\text{RO}}$  and  $k_a^{\text{RO}}$  and a dissociation equilibrium constant  $K_D^{\text{RO}}$  are determined for a single analyte molecule interacting with a single ligand molecule. Instead of using the response of loading RSPO1 to the anti-Flag spots ( $R_L$ ), the calculated  $R_{\text{max}}$  values can also be used for extrapolating the  $k_d$  and  $K_D$  values to zero response. The  $R_{\text{max}}$  value is the theoretical response value when all ligand molecules are saturated with analyte molecules. The ratio of the calculated  $R_{\text{max}}$  and  $R_L$  is constant and is proportional to the molecular weights:  $MW_{\text{LGR5-exo-Fc}}/MW_{\text{RSPO1-FH}} = R_{\text{max}}/R_L$ . A cross-check was performed by comparing the ratio of the calculated  $R_{\text{max}}$  and the experimentally determined  $R_L$  for extrapolation of  $R_L$  to zero. The ratio of approximately 5 that was obtained for low values of ligand density and low analyte concentrations indeed corresponds with the molecular weight ratio, which is 177 kDa for LGR5-exo-Fc (dimer) and 35 kDa for RSPO1-FH.

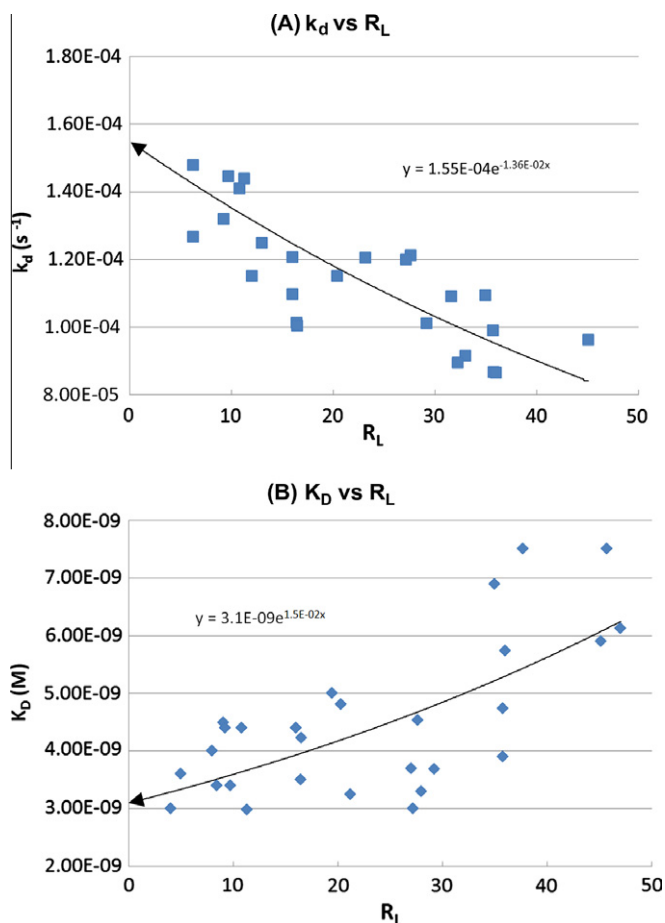


**Fig. 2.** Plots of the apparent  $k_d$  (A) and  $K_D$  (B) calculated values using a 1:1 binding model from serial injections of LGR5-exo-Fc to the array of RSP01-FH captured spots as measured in the IBIS MX96 biosensor instrument. In IBIS SPrint software (version 2), the exponential fitting routine  $y = a^x e^{bx}$  was used for determination of the values of  $k_d^{RO}$  and  $K_D^{RO}$  when  $R_L$  was extrapolated to zero (arrow). The coefficient of the exponential  $a$  (y intercept) resulted in  $k_d^{RO} = 1.55 \times 10^{-4} \text{ s}^{-1}$  and  $K_D^{RO} = 3.1 \times 10^{-9} \text{ M}$  ( $k_a^{RO} = 5.0 \times 10^4 \text{ M}^{-1} \text{ s}^{-1}$ ) for binding of the LGR5-exo-Fc to RSP01-FH.

Fig. 2A shows a typical downward trend of  $k_d$  versus  $R_L$ , and Fig. 2B shows an upward trend for  $K_D$  versus  $R_L$ . These trends are due to the already mentioned interferences. Without revealing the contribution of these interfering effects, which are nonlinear in nature, it was recognized that ligand densities should be as low as possible to approach the true “solution” single molecular

affinity constants. For calculation of the real affinity constants, the contribution of the lower analyte concentrations to low ligand density spots should be more dominant (e.g., a better approach of the interaction in solution), and the exponential fitting to zero response will approach this. The data were analyzed using a classical global 1:1 interaction model (See Fig. S1) and, therefore, were intrinsically validated. The values range from  $3 \times 10^{-9}$  to  $8 \times 10^{-9} \text{ M}$  for  $K_D$  and from  $8 \times 10^{-5}$  to  $1.5 \times 10^{-4} \text{ s}^{-1}$  for  $k_d$ . Comparison indicates that interfering effects have a significant impact on the true value of the dissociation equilibrium and rate constants. With the new method, the  $K_D^{RO}$  and  $k_d^{RO}$  for the interaction of LGR5-exo-Fc with RSP01-FH are determined to be  $3.1 \times 10^{-9} \text{ M}$  and  $1.55 \times 10^{-4} \text{ s}^{-1}$ , respectively

### Acknowledgment

Marc Bijen and Marcel Horsthuis of IBIS Technologies are acknowledged for development of the liquid handling procedures and for data processing by SPrint 2.0 software.

### Appendix A. Supplementary data

Supplementary data associated with this article can be found, in the online version, at [doi:10.1016/j.ab.2011.12.011](https://doi.org/10.1016/j.ab.2011.12.011).

### References

- [1] R.B.M. Schasfoort, A.J. Tudos (Eds.), Handbook of Surface Plasmon Resonance, Royal Society of Chemistry, London, 2008, p. 284.
- [2] D.G. Myszka, X. He, M. Dembo, T.A. Morton, B. Goldstein, Extending the range of rate constants available from BIACORE: interpreting mass transport-influenced binding data, *Biophys. J.* 75 (1998) 583–594.
- [3] P. Schuck, P.H. Zhao, The role of mass transport limitation and surface heterogeneity in the biophysical characterization of macromolecular binding processes by SPR biosensing, *Methods Mol. Biol.* 627 (2010) 15–54.
- [4] W. de Lau, N. Barker, T.Y. Low, B.-K. Koo, V.S.W. Li, H. Teunissen, P. Kujala, A. Haegebarth, P.J. Peters, M. vande Wetering, D.E. Stange, J. van Es, D. Guardavaccaro, R.B.M. Schasfoort, Y. Mohri, K. Nishimori, S. Mohammed, A.J.R. Heck, H. Clevers, Lgr5 homologs associate with Wnt receptors and mediate R-spondin signalling, *Nature* 476 (2011) 293–297.
- [5] Q. Wei, C. Yokota, M.V. Semenov, B. Doble, J. Woodgett, X. He, R-spondin1 is a high affinity ligand for LRP6 and induces LRP6 phosphorylation and  $\beta$ -catenin signaling, *J. Biol. Chem.* 282 (2007) 15903–15911.
- [6] A.M.C. Lokate, J.B. Beusink, G.A.J. Besselink, G.J.M. Pruijn, R.B.M. Schasfoort, Biomolecular interaction monitoring of autoantibodies by scanning surface plasmon resonance microarray imaging, *J. Am. Chem. Soc.* 129 (2007) 14013–14018.
- [7] J.B. Beusink, A.M.C. Lokate, G.A.J. Besselink, G.J.M. Pruijn, R.B.M. Schasfoort, Angle-scanning SPR imaging for detection of biomolecular interactions on microarrays, *Biosens. Bioelectron.* 23 (2008) 839–844.
- [8] S. Natarajan, P.S. Katsamba, A. Miles, J. Eckman, G.A. Papalia, R.L. Rich, B.K. Gale, D.G. Myszka, Continuous-flow microfluidic printing of proteins for array-based applications including surface plasmon resonance imaging, *Anal. Biochem.* 373 (2008) 141–146.